Molecular assessment of complex microbial communities degrading long chain fatty acids in methanogenic bioreactors

Diana Z. Sousa[1,2], M. Alcina Pereira[1,2], Hauke Smidt[2], Alfons J.M. Stams[2] & M. Madalena Alves[1]

[1]Center of Biological Engineering, University of Minho, Campus de Gualtar, Portugal; and [2]Laboratory of Microbiology, Wageningen University, Wageningen, The Netherlands

Correspondence: Madalena Alves, Center of Biological Engineering, University of Minho, Campus de Gualtar, 4710-057 Braga, Portugal. Tel.: +351 25360 4402; fax: +351 25367 8986; e-mail: madalena.alves@deb.uminho.pt

Received 29 May 2006; revised 18 October 2006; accepted 2 December 2006.
First published online 20 March 2007.

DOI:10.1111/j.1574-6941.2007.00291.x

Editor: Michael Wagner

Keywords
anaerobic digestion; LCFA; microorganisms; molecular tools.

Abstract

Microbial diversity of anaerobic sludge after extended contact with long chain fatty acids (LCFA) was studied using molecular approaches. Samples containing high amounts of accumulated LCFA were obtained after continuous loading of two bioreactors with oleate or with palmitate. These sludge samples were then incubated in batch assays to allow degradation of the biomass-associated LCFA. In addition, sludge used as inoculum for the reactors was also characterized. Predominant phylotypes of the different samples were monitored using denaturing gradient gel electrophoresis (DGGE) of PCR-amplified 16S rRNA gene fragments. Fingerprinting analysis showed changes in bacterial and archaeal communities during LCFA accumulation and degradation. Full-length 16S rRNA gene sequences of 22 clones, representing the predominant bacteria and archaea, were determined. Most bacterial clones (80%) clustered within the *Clostridiaceae*. Two major groups of methanogens were identified: hydrogen- and formate-utilizing organisms, closely related to *Methanobacterium*, and acetoclastic organisms closely related to *Methanosaeta* and *Methanosarcina*. Quantification by FISH and real-time PCR showed that the relative abundance of archaea increased during degradation of biomass-accumulated LCFA. These results provide insight into the importance and dynamics of balanced communities of bacteria and methanogens in LCFA-accumulation/degradation cycles.

Introduction

Anaerobic digestion has been extensively and successfully applied in wastewater treatment for the last decades. At present, the value of this process has gained an important position in view of the increased interest in renewable energy sources, since it combines the removal of organic pollutants from wastewaters with energy conservation in the form of the production of biogas. The energy yield of this process depends on the organic matter present in the wastewater and is especially elevated for highly reduced compounds, such as long chain fatty acids (LCFA). LCFA are frequently found in wastewaters, as the main product of lipid hydrolysis, and have been associated with toxic and bactericidal effects for years (Koster & Cramer, 1987; Angelidaki & Ahring, 1992; Rinzema *et al.*, 1994; Hwu, 1997). Their removal from the wastewater by physico-chemical processes prior to anaerobic treatment is a common practice, with consequent loss of a high energetic potential. Recently, the authors were able to show that the adverse effects of LCFA on anaerobic sludge functionality are not irreversible and that anaerobic sludge, under the appropriate conditions, was able to efficiently mineralize them (Pereira *et al.*, 2003, 2004). Cycles of continuous feeding of lipid/LCFA-rich wastewaters followed by batch degradation of the accumulated substrate might be an appropriate way to treat this type of wastewater.

LCFA are primarily degraded via β-oxidation with the production of acetate and hydrogen (Weng & Jeris, 1976). These compounds are further converted to methane and carbon dioxide. The overall conversion involves the concerted action of fatty acid oxidizing bacteria and methanogens that utilize hydrogen and acetate (Schink, 1997). Thus far, 10 bacterial species and subspecies have been characterized that grow on fatty acids with more than four carbon atoms and up to 18 carbon atoms in syntrophic association with methanogens. They all belong to the families *Syntrophomonadaceae* within the group of low G+C-containing Gram-positive bacteria (McInerney, 1992; Zhao *et al.*, 1993;

Wu *et al.*, 2006), or *Syntrophaceae* in the subclass of the *Deltaproteobacteria* (Jackson *et al.*, 1999). Hydrogenotrophic microorganisms control the redox potential of the media, maintaining hydrogen concentration at low levels, and thus conditioning syntrophic acetogenesis. This trophic group includes a large number of species within 5 orders in the archaea (Hedderich & Whitman, 2005). In a recent survey, *Methanobacterium* spp. were identified as the most frequent hydrogenotrophs present in 44 different anaerobic digesters (Leclerc *et al.*, 2004). Only a limited number of acetoclastic archaea has been isolated, all belonging to *Methanosaeta* (three species, homotrophic) and *Methanosarcina* (seven species, some can also utilize H_2 and CO_2, methylated amines and methanol) genera (Elberson & Sowers, 1997; Kendall & Boone, 2004; Ma *et al.*, 2006). Using samples from a variety of bioreactors, Zheng & Raskin (2000) demonstrated that *Methanosaeta* spp. are the dominant acetoclastic methanogens at low acetate concentrations. In the same study, *Methanosarcina* spp. outcompeted *Methanosaeta* spp. when acetate concentrations were high. These findings are in accordance with the kinetic growth parameters for these two groups, as *Methanosaeta* spp. have higher affinities for acetate but lower growth rates than *Methanosarcina* spp. (Jetten *et al.*, 1992).

Insight in abundance and phylogenetic affiliation of microorganisms involved in LCFA degradation can be investigated by molecular 16S rRNA gene-targeting techniques. Microbial community fingerprinting by denaturing gradient gel electrophoresis (DGGE), cloning and sequencing analysis, and FISH are suitable cultivation-independent tools for the analysis of complex microbial communities (Amann *et al.*, 1995). Pereira *et al.* (2002) used a combination of different molecular techniques to analyze the microbial diversity of bacteria and archaea in two bioreactors inoculated with granular and suspended sludge and fed with increasing concentrations of oleate. The communities in reactors treating LCFA-rich wastewaters are rather diverse and complex. A large number of not-yet-cultured bacteria belonging to *Firmicutes* (low G+C Gram-positive bacteria) and *Proteobacteria* was detected. In the present study microbial communities present in sludge loaded with LCFA, collected from reactors continuously fed with oleate and palmitate, and sludge samples after depletion in batch reactors of the accumulated LCFA, were analyzed by comparative sequence analysis of 16S rRNA genes, amplified from total community genomic DNA. For comparison, a sample taken from the reactors' inoculum was also analyzed. The aim was to identify LCFA-degrading bacteria present in anaerobic bioreactors treating LCFA-rich wastewaters and get more insight into the composition of syntrophic LCFA-degrading communities, using culture-independent techniques.

Materials and methods

Sludge sources

A total of five anaerobic sludge samples, designated as I, SO, SP, SO_b and SP_b, were used in this study. Suspended sludge, obtained from a local municipal sludge digester (Braga ETAR, Portugal) was acclimated to oleate in the presence of skim milk as cosubstrate (50% COD). Analysis of the free LCFA present in skim milk showed that palmitate ($C_{16:0}$) is the main free LCFA present, representing 32–48% of the total LCFA. Myristate ($C_{14:0}$), stearate ($C_{18:0}$) and oleate ($C_{18:1}$) were also detected, corresponding to 11–15%, 7–17% and 23–26% of the total LCFA, respectively (Cavaleiro & Alves, unpublished data). The acclimation procedure was carried out in a 4-L fed-batch reactor, at $37 \pm 1\ ^\circ C$, and using substrate concentrations of 1–2 g COD L^{-1}. Acclimated sludge was used as inoculum (sample I) for two 1-L expanded granular sludge bed (EGSB) reactors. These two reactors, designated RO and RP, were continuously fed during 75 days with oleate and palmitate, respectively, as described previously (Pereira *et al.*, 2005). The following operating conditions were used for the reactors: the influent LCFA concentration was 4 (g COD) L^{-1}, the HRT was set at 1 day, and the temperature was 37 °C. Floating sludge was recycled to the influent port at a rate of 4 L day^{-1}. During the continuous operation, only a slow degradation of the fed LCFA was achieved in both reactors, with methane yields as low as 33 and 29 (L CH_4) $(kg\ COD_{removed})^{-1}$ in RO and RP, respectively, resulting in a considerable accumulation of nonmineralized substrate (Pereira *et al.*, 2005). At the end of the continuous load, the sludge collected from RO and RP (samples SO and SP) exhibited specific LCFA contents of 4570 ± 257 and of 5200 ± 9 mg COD $gVSS^{-1}$, respectively (Pereira *et al.*, 2005). Palmitate was the main LCFA accumulated onto both sludges, representing 83% of the total LCFA present in the sludge collected from RO (sludge SO) and the totality of the LCFA present in the sludge collected from RP (sludge SP). The way of LCFA accumulation was different in the two sludges: in sludge SO the biomass-associated LCFA were mainly adsorbed and entrapped in the sludge that became 'encapsulated' by a LCFA layer, whereas sludge SP contained white precipitates in between the sludge, which remained 'nonencapsulated' (Pereira *et al.*, 2005). Subsequently, the biomass was washed and centrifuged (1681 ***g***, 10 min) twice with anaerobic basal medium. The basal medium was made up with demineralized water and contained 0.5 g L^{-1} cysteine-HCL and 3 g L^{-1} sodium bicarbonate, and the pH was adjusted to 7.0–7.2 with NaOH 8 N and was prepared under strict anaerobic conditions. Each LCFA-loaded sludge was then incubated in anaerobic batch assays with the same anaerobic basal medium. Incubation was carried out at 37 °C, while stirring was carried out at

150 r.p.m., to allow degradation of the biomass-associated LCFA (Pereira *et al.*, 2005). In both sludges, the process lasted *c.* 800 h, after which methane production ceased and samples from both sludges were collected (samples SO_b and SP_b).

DNA extraction and amplification

Approximately 1-mL aliquots of well-homogenized sludge were immediately frozen at the time of sampling and stored at −20 °C, and total genomic DNA was extracted using a FastDNA SPIN Kit for Soil (Qbiogene, Carlsbad, CA).

The 16S rRNA-genes were amplified by PCR using a *Taq* DNA Polymerase kit (Life Technologies, Gaithersburg, MD) with primers targeting conserved domains. PCR reaction mixtures consisted of 20 mM Tris-HCl (pH 8.4), 50 mM KCl, 3 mM $MgCl_2$, 200 μM each of the four deoxynucleoside triphosphates (dNTP), 2.5 U of *Taq* polymerase, 200 nM of each primer and 1 μL of appropriately diluted template DNA in a final volume of 50 μL. All primers used were synthesized commercially by MWG-Biotech (Ebersberg, Germany) and are listed in Table 1.

Bacterial and archaeal 16S rRNA genes were selectively amplified for cloning using the forward primers Bact27-f and Arch109-f, respectively, and the universal reverse primer Uni1492-r. For both domains the thermocycling program used for amplification was as follows: predenaturation at 95 °C for 5 min; 25 cycles of denaturation at 95 °C for 30 s, annealing at 52 °C for 40 s and elongation at 72 °C for 90 s, and postelongation at 72 °C for 5 min. The reactions were subsequently cooled to 4 °C.

For DGGE analysis, PCR products were generated using bacterial 16S rRNA gene primers U968-f and L1401-r, targeting the V6–V8 region, and primers A109(T)-f and 515-r for amplification of the archaeal V2 to V3 region. Primers U968-f and 515-r were modified by the addition of a 40 bp GC clamp at the 5′ end of the sequence (Table 1). The program for amplification was as described above but with 35 cycles and an annealing temperature of 56 °C.

Size and yield of PCR products were estimated using a 100 bp DNA ladder (MBI Fermentas, Vilnius, Lithuania) via 1% (w/v) agarose gel electrophoresis and ethidium bromide staining.

DGGE analysis

DGGE analysis of the amplicons was performed as previously described by Zoetendal *et al.* (2001), using the Dcode system (Bio-Rad, Hercules, CA) with 8% (v/v) polyacrylamide gels and a denaturant gradient of 30–60%.

Table 1. Oligonucleotides used in this study

Oligonucleotide	Sequence (5′–3′)	Specificity	Reference or source
Bact27-f*	GTT TGA TCC TGG CTC AG	Bacterial 16S	Lane (1991)
Arch109-f*	ACK GCT CAG TAA CAC GT	Archaeal 16S	Grosskopf *et al.* (1998)
Uni1492-r*	CGG CTA CCT TGT TAC GAC	Universal 16S	Lane (1991)
U968-f*	AAC GCG AAG AAC CTT AC	Bacterial 16S	Nübel *et al.* (1996)
L1401-r*	CGG TGT GTA CAA GAC CC	Bacterial 16S	Nübel *et al.* (1996)
A109(T)-f*	ACT GCT CAG TAA CAC GT	Archaeal 16S	Original Grosskopf *et al.* (1998), but with third nucleotide changed into T
515-r*	ATC GTA TTA CCG CGG CTG CTG GCA	Universal 16S	Lane (1991)
GC clamp	CGC CCG GGG CGC GCC CCG GGC GGG GCG GGG GCA CGG GGG G		Muyzer *et al.* (1993)
PG2-r	GGC CGC GAA TTC ACT AGT G	pGEM-T	Promega Corp.
PG1-f	TGG CGG CCG CGG GAA TTC	pGEM-T	Promega Corp.
T7	TAA TAC GAC TCA CTA TAG GG	pGEM-T	Promega Corp.
SP6	GAT TTA GGT GAC ACT ATA G	pGEM-T	Promega Corp.
Uni533-f*	GTG CCA GC(A/C) GCC GCG GTA A	Universal 16S	Lane (1991)
Bact1100-r*	GGG TTG CGC TCG TTG	Bacterial 16S	Lane (1991)
Arch907-r*	CCG TCA ATT CCT TTG AGT TT	Archaeal 16S	Lane (1991)
BAC338-f *	ACT CCT ACG GGA GGC AG	Bacterial 16S	Yu *et al.* (2005b)
BAC805-r*	GAC TAC CAG GGT ATC TAA TCC	Bacterial 16S	Yu *et al.* (2005b)
ARC787-f *	ATT AGA TAC CCS BGT AGT CC	Archaeal 16S	Yu *et al.* (2005b)
ARC1059-r*	GCC ATG CAC CWC CTC T	Archaeal 16S	Yu *et al.* (2005b)
ARCH915†	GTG CTC CCC CGC CAA TTC CT	Archaea	Stahl & Amann (1991)
NON338†	ACT CCT ACG GGA GGC AGC	Antisense of EUB338	Wallner *et al.* (1993)

*16S rRNA gene primer.

†16S rRNA probe labeled with Cy5.

A 100% denaturing solution was defined as 7 M urea and 40% formamide. Electrophoresis was performed for 16 h at 85 V in a 0.5 × TAE buffer at 60 °C. DGGE gels were stained with $AgNO_3$ as described (Sanguinetti *et al.*, 1994), scanned at 400 dpi, and the DGGE profiles were compared using the BIONUMERICS™ software package (version 4.0; Applied Maths BVBA, Sint-Martens-Latem, Belgium). Similarity indices of the compared profiles were calculated from the densitometric curves of the scanned DGGE profiles using the Pearson product-moment correlation coefficient. According to Hane *et al.* (1993), the Pearson product-moment correlation coefficient is better suited for the identification of fingerprints than band matching algorithms. The Pearson correlation coefficient is directly applied to the array of densitometric values forming the fingerprint. The coefficient is robust and objective, since whole curves are compared and subjective band scoring is omitted. Clustering of patterns was calculated using the unweighted-pair group method using arithmetic mean (UPGMA).

Cloning and sequencing of PCR-amplified products

PCR amplicons were purified with the QIAquick PCR purification kit (Qiagen GmbH, Hilden, Germany) according to the manufacturer's instructions, and cloned into *Escherichia coli* JM109 (Invitrogen, Breda, the Netherlands) using the Promega pGEM-T Easy vector system (Promega, Madison, WI). PCR was performed on cell lysates of ampicillin-resistant transformants using pGEM-T specific primers PG1-f and PG2-r (Table 1) to confirm the size of the inserts. Amplicons of the correct size were screened by amplified ribosomal DNA restriction analysis (ARDRA), using the restriction enzymes MspI, CfoI and AluI (Promega, Madison, WI); acetylated bovine serum albumin (BSA) was added to the digestion reaction to a final concentration of 0.1 mg mL^{-1}. The restriction fragments were analyzed by electrophoresis in a 4% (w/v) agarose gel and visualized with ethidium bromide. Plasmids of selected transformants, with different ARDRA patterns and corresponding to predominant bands in the DGGE community fingerprint, were purified using the QIAquick PCR purification kit (Qiagen, Hilden, Germany) and subjected to DNA sequence analysis. Sequencing reactions were performed at Westburg Genomics (Leusden, the Netherlands) using pGEM-T vector-targeted sequencing primers, SP6 and T7, and 16S rRNA-gene-targeted internal primers, Uni533-f and Bact1100-r or Arch907-r for bacterial or archaeal 16S rRNA gene amplification, respectively (Table 1). Consensus sequences obtained were checked for potential chimera artifacts by the CHECK_CHIMERA program of the Ribosomal Database Project II (RDP release 8.1, http://rdp8.cme.msu.edu/html/) (Cole *et al.*, 2003).

Phylogenetic analysis

Similarity searches for the 16S rRNA gene sequences derived from the sludge clones were performed using the NCBI BLAST search program within the GenBank database (http://www.ncbi.nlm.nih.gov/blast/) (Altschul *et al.*, 1990).

Alignment of the 16S rRNA gene sequences was performed using the FASTALIGNER V1.03 tool of the ARB program package (Ludwig *et al.*, 2004). The resulting alignments were manually checked and corrected when necessary, and unambiguously aligned nucleotide positions were used for construction of archaea and bacteria 16S rRNA gene based phylogenetic trees, using the neighbour-joining method (Saitou & Nei, 1987). Phylogenetic placement was performed in comparison with reference sequences with Felsenstein correction and application of appropriated filters at the respective phylum level.

Nucleotide sequences obtained in this study have been deposited in the GenBank database under accession numbers DQ339700–DQ339721.

Quantitative real-time PCR

Real-time PCR quantification of archaea and bacteria in sludge samples was carried using the iQ5 real-time PCR detection system and the iQ SYBR Green Supermix Kit (Bio-Rad, Hercules, CA). Individual real-time PCR reactions were performed in a total volume of 25 μL, consisting of 12.5 μL iQ SYBR Green Supermix, 0.5 μL of both the forward and reverse primers (200 nM final concentration), 6.5 μL of PCR-grade deionized water and 5 μL of template DNA. Amplification of bacterial or archaeal 16S rRNA genes was performed using the primer pairs BAC338-f/BAC805-r and ARC787-f/ARC1059-r, respectively. Primers were purchased from MWG-Biotech (Ebersberg, Germany) and are listed in Table 1. A control reaction without template DNA was included in each real-time PCR assay. All DNA samples and the negative control were analyzed in quadruplicate. For real-time PCR of bacteria the thermocycling program used was as follows: 10 min at 95 °C for initial heat activation, followed by 45 cycles of denaturation for 15 s, annealing at 60 °C for 30 s and extension at 72 °C for 30 s. For archaea the annealing and extension steps were combined in one step at 60 °C for 30 s. Real-time fluorescence data were obtained at the end of each PCR cycle, and after the PCR cycles melting curves were acquired and analyzed. Subsequently, the threshold value for fluorescence was manually set at the lowest possible level at which exponential amplification occurred for all reactions. The PCR-cycle at which the fluorescence in a reaction crossed this threshold (threshold cycle: C_t) was then automatically determined. Standard curves were automatically generated by the IQ5 software, based on C_t-values corresponding to a 10-fold dilution series (10^9–10^2 copies). DNA-samples for standard

curves were prepared by amplifying group-specific full-length 16S rRNA genes, cloned in vector pGEM®-T Easy (Promega, Madison, WI), using vector-targeted primers T7 and SP6 (Table 1), and PCR products purified with the NucleoSpin® Extract II Kit (Macherey-Nagel, Düren, Germany). DNA-standards were quantified with a Nanodrop spectrophotometer, and copy-numbers in the unknown samples were automatically calculated based on the standard curve.

Cell fixation and FISH

Immediately after sampling, sludge samples were washed and resuspended in phosphate-buffered saline (PBS) and fixed overnight according to Amann (1995). Fixed samples were washed twice with PBS and stored in PBS/ethanol (1 : 1) at $-20\,^{\circ}C$ until further processing. Samples were then dispersed by sonication for 2×1 min at 150 Watt and dilution series prepared in PBS/ethanol in order to determine the optimal cell concentration for counting. Fixed cells were spotted to wells on gelatine-coated slides, dried for 20 min at 45 °C and dehydrated in a graded ethanol series (Amann, 1995). *In situ* hybridization was performed as described by Manz *et al.* (1992), using the oligonucleotide probe ARCH915 (Table 1). For total counts, 4,6 diamidino-2-phenylindole (DAPI) was added to the wash buffer at a final concentration of 100 ng mL^{-1}. After rinsing the slides in water, they were immediately dried and mounted in Vectashield (Vector Labs, Burlingame, CA). All preparations were performed in triplicate. Digital images of the slides were viewed with a Leica (Wetzlar, Germany) DMR HC epifluorescence microscope. Pictures were taken with a Leica DC 250 digital camera. Quantification of the fluorescent cells was carried out using LEICA QWIN software according to the manufacturer's instructions (Leica Microsystems, Rijswijk, the Netherlands). Cells were counted in 10 microscopic fields randomly selected across each well section. Between 2000 and 3000 DAPI-stained cells were counted per sample. Counting results were verified and corrected by subtracting signals observed with the negative control, in which the nonsense probe NON338 was used (Table 1). Statistical evaluation of the obtained data was carried out with the software STATISTICA (version 4.0; StatSoft, São Caetano do Sul, Brazil). The Kruskal–Wallis nonparametric test (nonparametric analogous to the F-test used in ANOVA) was used to confirm that replicate subsets data were statistically indistinguishable and, thus, drawn from the same population. The statistical significance of the differences detected between pairs of different sludge sample data sets was evaluated using the Mann–Whitney *U*-test (analogous nonparametric test for a two-sample *t*-test or a single-way ANOVA for two samples). Statistical significance was established at the $P < 0.05$ level for each analysis.

Results

Microbial community pattern of sludges during LCFA accumulation and degradation

Microbial diversity and shifts in bacterial and archaeal communities present in the samples were estimated based on the DGGE patterns of the partial 16S rRNA gene amplicons. A total of five sludge samples were compared: samples containing a high amount of accumulated LCFA, SO and SP, obtained after a continuous load in two EGSB reactors with oleate and palmitate, respectively; the suspended sludge used as inoculum for both reactors, sample I; and samples SO_b and SP_b, obtained after batch incubation of sludge SO and SP, respectively, to allow the degradation of the accumulated LCFA.

The analysis of DGGE band-patterns from the sludge samples revealed a clear shift in the microbial consortium through the LCFA accumulation and degradation steps (Fig. 1). During LCFA accumulation, this shift was more pronounced in the bacterial community structure, as indicated by the comparison of the calculated similarity indices. Bacterial similarity between the sludge loaded with oleate (SO) and the inoculum (I) was 23.5%, and between the sludge loaded with palmitate (SP) and the inoculum 34.9%, whereas for the archaeal domain the similarity indices were 95.2% and 96.8%, respectively. At the end of the continuous operation, the sludges of both reactors exhibited almost identical archaeal profiles (similarity index of 99.0%), while the bacterial communities exhibited significant differences at a similarity of 54.0%. The high similarity of the archaeal communities present in the LCFA-loaded sludge samples (SO and SP) and the inoculum indicates that archaeal composition remained rather stable during the continuous LCFA load. However, this was not the case during the batch degradation step. After batch degradation of the LCFA accumulated onto the sludge, the archaeal profiles of both depleted sludge samples (SO_b and SP_b) exhibited a similarity index towards the correspondent LCFA-loaded sludges of only 37.0% and 6.2%, respectively. At this time point, the bacterial similarity index between sludge SO_b and SO was 60.7%, and between sludge SP_b and SP was 74.6%, indicating that the prevailing bacterial community structure was less affected by the batch degradation step.

Phylogenetic analyses of predominant bands in the DGGE patterns

To assign the composition of the predominant community visualized in the DGGE-patterns, nearly full-length bacterial and archaeal 16S rRNA gene fragments, retrieved from the five sludge samples, were used to construct clone libraries. Clones with the same electrophoretic mobility as that of predominant bands of the bacterial and archaeal DGGE

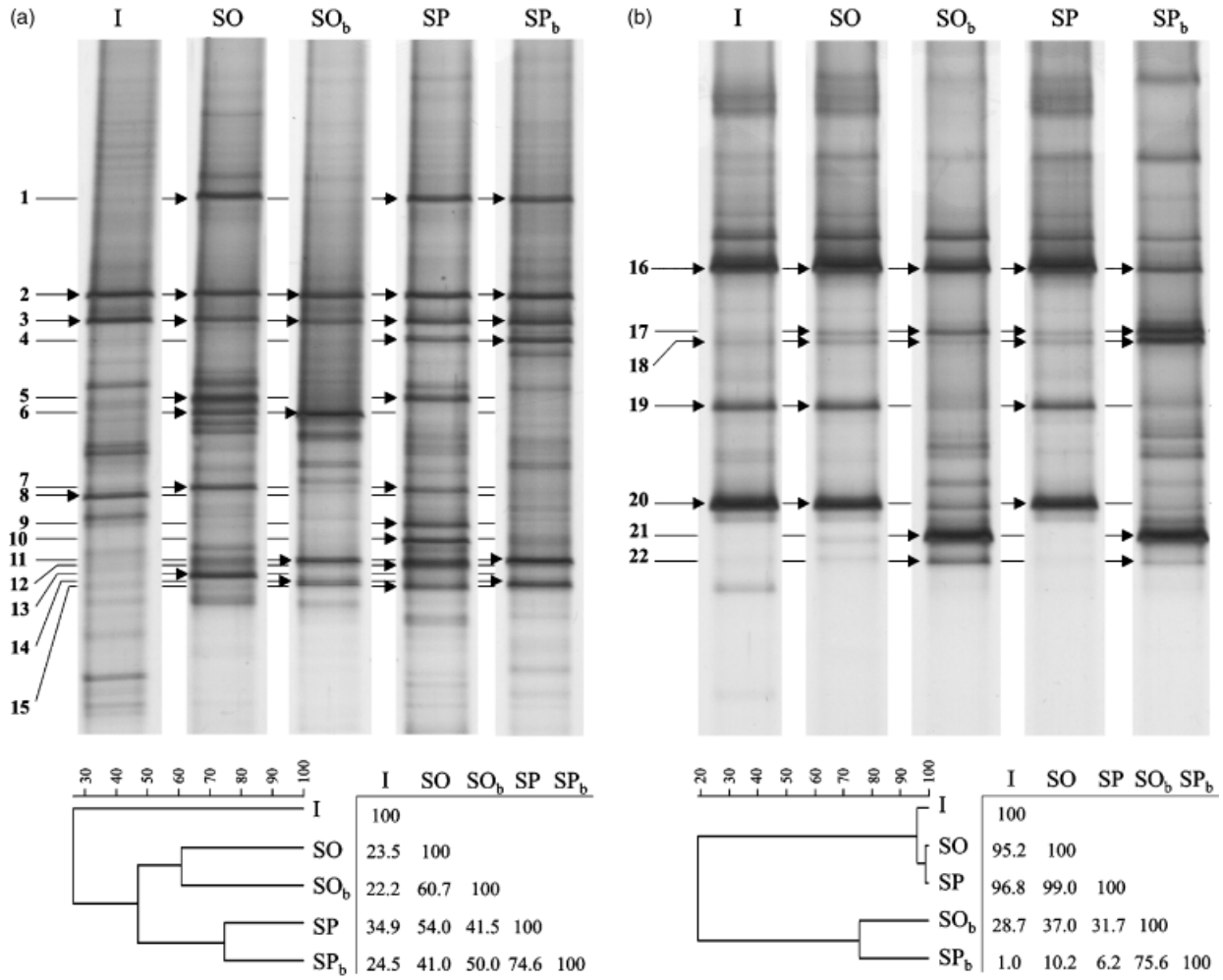

Fig. 1. DGGE patterns of (a) bacterial and (b) archaeal amplicons from the sludge samples: I, inoculum; SO, after continuous load in EGSB reactor with oleate; SP, after continuous load in EGSB reactor with palmitate; SO_b, SO after degradation of accumulated LCFA in batch; SP_b, SP after degradation of accumulated LCFA in batch. Corresponding similarity index dendrograms (UPGMA clustering) and similarity matrices are also presented. Numbered DGGE bands (1–22) were further identified by cloning and sequencing. Reproducibility of PCR-DGGE data, for each sample, was verified in independent experiments (data not shown).

patterns (bands 1–22, Fig. 1) were selected for further sequence analysis. Phylogenetic affiliation of sequences was initially assessed by BLAST similarity searches, and confirmed by secondary structure-assisted alignment and phylogenetic analysis (Table 2, Fig. 2).

The majority of sequences obtained from clones corresponding to predominant DGGE-bands clustered within the *Firmicutes* (13/15 sequences, 87%), among which members of the *Clostridiaceae* (bands 1, 2, 4, 5 and 14, Table 2) and *Syntrophomonadaceae* (bands 6, 10, 11 and 15, Table 2) families represented 69% (9/13 sequences). A significant part of the retrieved bacterial 16S rRNA gene sequences (53%) were most similar to those of yet uncultured microorganisms, with the majority assigned to the phylum *Firmicutes* (6/8 sequences; 75%). Members of *Proteobacteria* and *Bacteroidetes* were also found among these sequences, though with only one representative for each phylum, and not detectable in DGGE profiles from samples after batch degradation. Some of the predominant bands in the DGGE profile of the inoculum sludge (I) became practically undetectable in the DGGE profiles of the sludges submitted to an extensive contact with LCFA. This was the case for clone lcfa_B05 (corresponding to band 8, Table 2), closely related to *Eubacterium callanderi*. In contrast, bands corresponding to two sequences closely related to *Clostridium* species (bands 2 and 3, Table 2) did not significantly change in intensity through accumulation/degradation steps, suggesting that these bacteria were functionally present in all the analyzed samples. Furthermore, other *Clostridium*-like bacteria appeared as predominant bands in the different

Table 2. Affiliation of the retrieved bacterial (clones 1–15) and archaeal (clones 16–22) clones

						Predominant band present in				
Band ID	Clone	Closest relative (> 1200 bp)	% Identity	Phylum	Accession nos.	I	SO	SO_b	SP	SP_b
1	lcfa Bc84	*Clostridium sp* 45	99	*Firmicutes*	DQ339700		•		•	•
2	lcfa Bb22	*Clostridium butyricum*	99	*Firmicutes*	DQ339701	•	•	•	•	•
3	lcfa Bc95	Uncultured bacterium clone C118	96	*Firmicutes*	DQ339702	•	•	•	•	•
4	lcfa Bb93	Uncultured bacterium clone p-2117-s959-2	99	*Firmicutes*	DQ339703				•	•
5	lcfa Bc73	*Clostridium propionicum*	99	*Firmicutes*	DQ339704		•		•	
6	lcfa Bb13	Uncultured bacterium clone R6b2	94	*Firmicutes*	DQ339705		•	•		
7	lcfa Bc67	Uncultured bacterium H30	96	*Proteobacteria*	DQ339706		•		•	
8	lcfa B05	*Eubacterium callanderi*	89	*Firmicutes*	DQ339707	•				
9	lcfa Bc62	Uncultured bacterium Eub No 20	97	*Firmicutes*	DQ339708				•	
10	lcfa Bc53	Unidentified eubacterium clone vadinCA02	99	*Firmicutes*	DQ339709				•	
11	lcfa Bb11	*Syntrophomonas wolfei*	93	*Firmicutes*	DQ339710			•		•
12	lcfa Bc85	Uncultured bacterium clone TSAT05	99	*Firmicutes*	DQ339711				•	
13	lcfa Bc90	Uncultured bacterium clone PL-7B6	98	*Bacteroidetes*	DQ339712		•			
14	lcfa Bb20	*C. butyricum* (NCIMB8082)	94	*Firmicutes*	DQ339713			•		•
15	lcfa Bb67	*Syntrophomonas wolfei*	92	*Firmicutes*	DQ339714					
16	lcfa Ac06	*Methanobacterium formicicum* strain FCam	98	*Euryarchaeota*	DQ339715	•	•	•	•	•
17	lcfa Ab25	*Methanobacterium aarhusense*	97	*Euryarchaeota*	DQ339716		•	•	•	•
18	lcfa Ab57	*Methanobacterium formicicum* strain FCam	98	*Euryarchaeota*	DQ339717	•	•	•	•	•
19	lcfa A03	*Methanosaeta concilii*	99	*Euryarchaeota*	DQ339718	•	•		•	
20	lcfa A06	*Methanosaeta concilii*	99	*Euryarchaeota*	DQ339719	•	•		•	
21	lcfa Ab59	*Methanosarcina mazei* strain Goe1	99	*Euryarchaeota*	DQ339720			•		•
22	lcfa Ab67	*Methanosarcina mazei* strain Goe1	99	*Euryarchaeota*	DQ339721			•		•

samples after contact with LCFA (bands 1, 4, 5, 9 and 14, Table 2, Fig. 2a). Populations related to established LCFA-degrading bacteria belonging to the *Syntrophomonadaceae* were not detected in the DGGE profiles of the inoculum sludge (I), whereas they appeared as predominant bacteria in sludge samples after contact with LCFA (bands 6, 10, 11 and 15, Table 2, Fig. 2a).

For the archaeal domain, the retrieved 16S rRNA gene sequences exhibited a similarity higher than 97% to sequences of cultivated methanogenic species, all belonging to the phylum *Euryarchaeota*. They were represented by sequences closely related to those of hydrogenophilic and acetoclastic methanogens of the orders *Methanobacteriales* and *Methanosarcinales*, respectively. *Methanobacterium* (bands 16–18), *Methanosaeta* (bands 19 and 20) and *Methanosarcina* (bands 21 and 22) (Table 2) were the most predominant genera present in the analyzed samples. While hydrogenophilic *Methanobacterium*-like organisms were present in all sludge samples, *Methanosaeta*- and *Methanosarcina*-related populations did not occur together as predominant microorganisms in any of the samples analyzed (Fig. 1b). *Methanosaeta*-like organisms, strict acetoclastic methanogens, corresponded to strong bands in the DGGE profiles of the inoculum sludge (I) and after continuous LCFA loading (SO and SP), but became very faint (practically undetectable) after batch degradation of the accumulated LCFA (SO_b and SP_b). Rather, microorganisms most closely related to *Methanosarcina* became the predominant acetoclastic archaea present in SO_b and SP_b sludge community patterns.

Quantification by FISH and real-time PCR

Variation in the relative abundance of archaea in the sludge submitted to LCFA accumulation/degradation steps was also evaluated by FISH using the probe ARCH915 (Table 3). For sample SO, the nonsense probe highlighted clumps and not individual signals, likely a result from trapping and/or adsorption of the probe in the LCFA matrix that 'encapsulated' the sludge (as mentioned in 'Materials and methods'). Therefore, this sample was not considered for further analysis by FISH. To overcome this limitation, relative quantification of archaea and bacteria in the same sludge samples was achieved using real-time PCR targeting the 16S rRNA gene (Table 3).

Values of archaea relative abundance in the different sludge samples measured by FISH were considerably lower than the relative archaeal 16S rRNA gene copy numbers (Table 3). The ratio of ARCH915-hybridized cells to total DAPI-stained cells showed a statistically significant ($P < 0.01$, Mann–Whitney *U*-test analysis) decrease from 33.4 ± 3.6 (I) to 19.1 ± 1.4 (SP), after the continuous load with palmitate. Through real-time PCR estimation, however, the variation on the relative abundance of archaeal

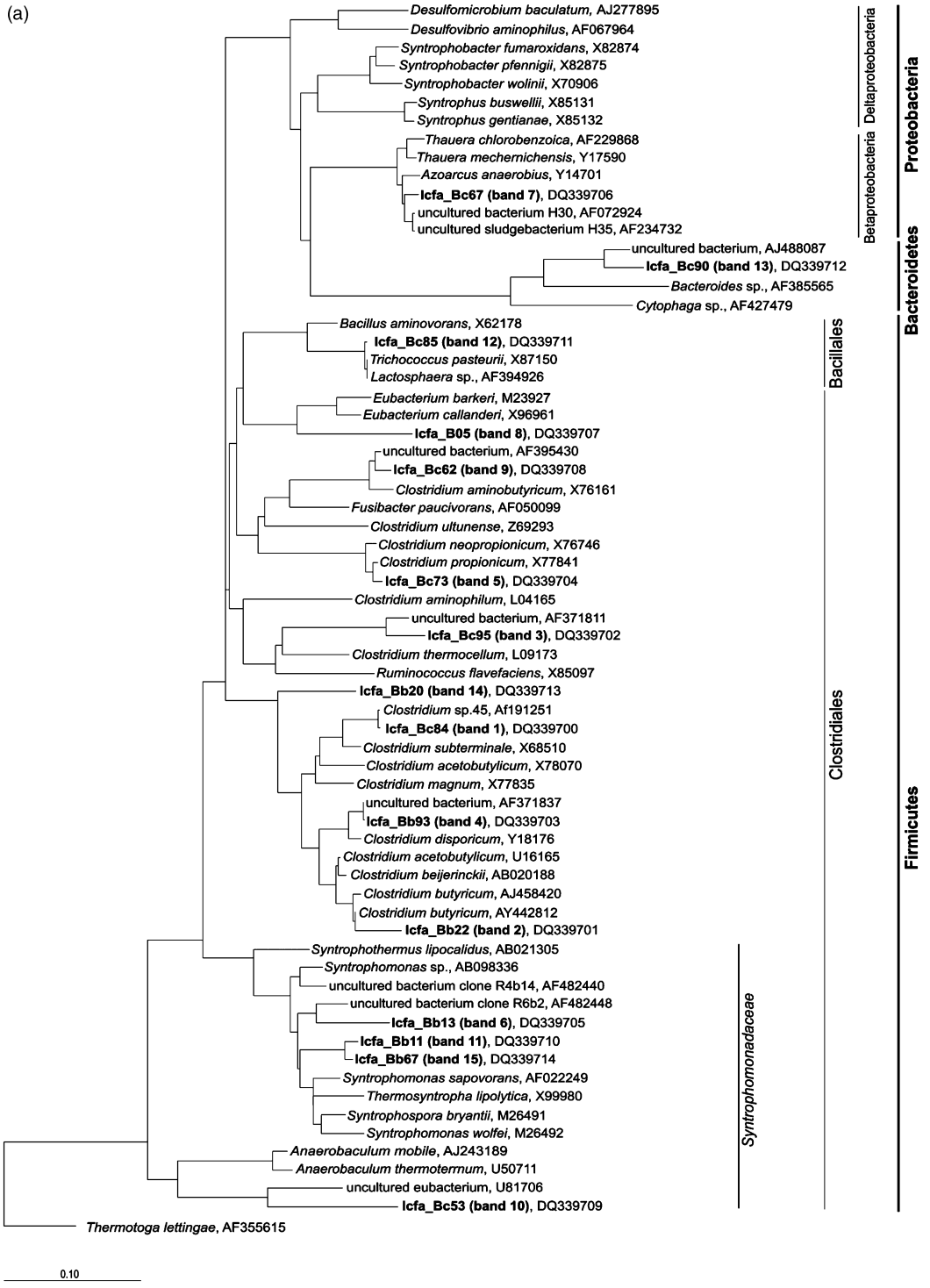

Fig. 2. Phylogenetic trees of (a) bacterial and (b) archaeal 16S rRNA gene sequences retrieved from the sludge samples: I, inoculum; SO, after continuous load in EGSB reactor with oleate; SP, after continuous load in EGSB reactor with palmitate; SO_b, SO after degradation of accumulated LCFA in batch; SP_b, SP after degradation of accumulated LCFA in batch. Trees were calculated using the ARB software package (Ludwig *et al*., 2004) and applying the neighbor-joining method (Saitou & Nei, 1987). Closely related sequences, with the respective Genbank accession number, are shown as reference. *Thermotoga lettingae* (AF355615) and *Pyrococcus furiosus* (U20163) were used as outgroup for bacteria and archaea trees, respectively. Reference bars indicate 10% sequence divergence.

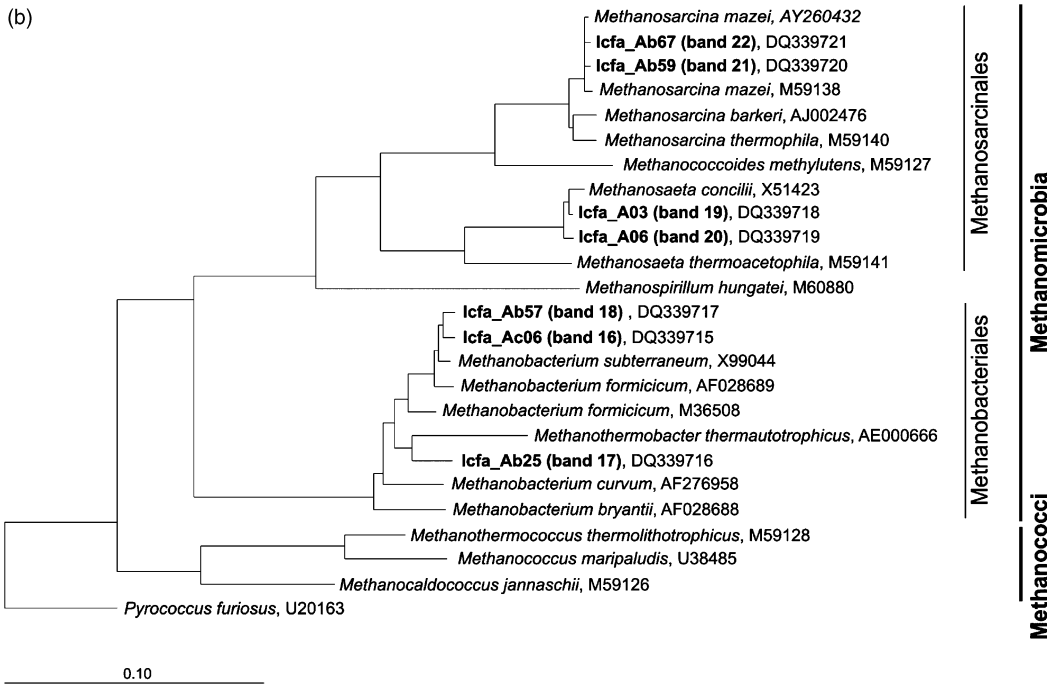

Fig. 2. Continued.

Table 3. Relative abundance of archaea in the samples under study, measured by 16S rRNA gene-targeted FISH and real-time PCR amplification of the corresponding gene

	Archaea relative abundance (%)				
	I	SO	SO_b	SP	SP_b
Archaea counts/DAPI counts	33.4 ± 3.6	ND	35.1 ± 1.7	19.1 ± 1.4	38.3 ± 6.2
Archaea copies/(archaea copies+bacteria copies)	42.4 ± 14.8	48.1 ± 9.0	85.3 ± 28.9	35.4 ± 14.3	75.0 ± 14.0

ND, not determined.

organisms induced in the inoculum sludge (I) by the continuous load with oleate (SO) and palmitate (SP) was found not to be significant. After the degradation of the accumulated LCFA in batch, the percentage of hybridized archaeal cells significantly increased ($P < 0.0001$, Mann–Whitney *U*-test analysis) from 19.1 ± 1.4 (SP) to 38.3 ± 6.2 (SP_b) of the total DAPI-stained cells. Similarly, real-time PCR measurements revealed a statistical significant increase ($P < 0.0001$, *t*-test analysis), of about twofold, in the relative abundance of archaeal microorganisms in the LCFA-depleted sample (SP_b) when compared to the correspondent LCFA-loaded sludge (SP). This increase was also detected when comparing samples SO and SO_b by real-time PCR.

Microscopic observations of the sludge samples hybridized with probe ARCH915 further confirmed the previous findings obtained by archaea-specific DGGE and cloning and sequencing. In the sludge obtained after allowing the degradation of the accumulated LCFA (SO_b and SP_b), *Methanosarcina*-shaped archaea were predominant whereas in the inoculum sludge (I) and after continuous LCFA loading (SP) this morphotype was not detected. Rather, *Methanosaeta*-shaped cells could be observed (Fig. 3). Morphologically the two genera are very distinct: *Methanosarcina* are generally cocci, which may occur singly, in packets, or in large pseudoparenchyma, whereas *Methanosaeta* include large sheathed rods, often forming long filaments and large aggregates (Kendall & Boone, 2004).

Discussion

Molecular characterization of sludge submitted to LCFA accumulation and subsequent degradation in batch incubations gave insight into the concomitant changes in the microbial composition as well as groups of microorganisms involved in this process. The comparison of the DGGE

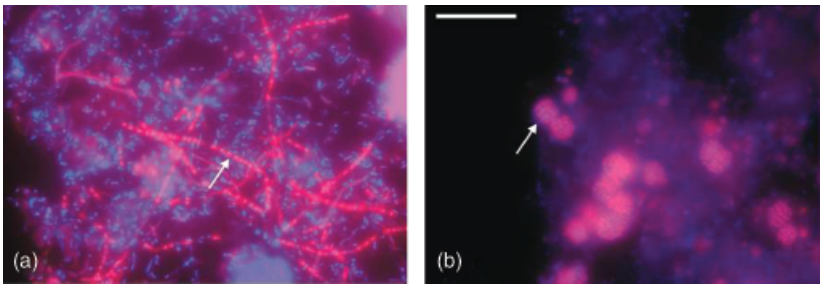

Fig. 3. Epifluorescence photographs showing *in situ* hybridization with probe ARCH915-Cy5 and DAPI-counterstaining of (a) sludge SP, after continuous load in EGSB reactor with palmitate and (b) SP_b, after allowing degradation in batch of accumulated LCFA (the aggregates were not dispersed by sonication). Arrows indicate *Methanosaeta*-like cells (a) and *Methanosarcina*-like cells (b). Bar = 10 μm.

band-patterns from sludge samples I, SO and SP revealed a significant shift in the composition of the bacterial community during the continuous load with LCFA (accumulation step). At the end of the continuous feeding, the bacterial community present in the reactors fed with oleate (RO) and palmitate (RP) exhibited a low resemblance (54.0% similarity between SO and SP). During the continuous load with LCFA the methane production in both reactors was very low, i.e. 33 and 29 L CH_4 (kg $COD_{removed}$)$^{-1}$ in RO and RP, respectively. In fact, most of the LCFA fed was accumulating onto both sludges and further conversion to methane was slow. Analysis of the accumulated substrate onto the sludge revealed that palmitate was the main LCFA present, representing 83% and 100% of the total accumulated LCFA onto the sludges SO and SP, respectively (Pereira *et al.*, 2005). This means that a first conversion step of oleate to palmitate takes place in reactor RO. The differences in the bacterial communities of samples SO and SP might be correlated with this additional conversion occurring only in reactor RO. In fact, the sequence of reactions involved in unsaturated-LCFA degradation is still not unambiguously resolved. Weng & Jeris (1976) proposed that the degradation of oleate starts with chain saturation by hydrogenation, leading to the formation of stearate. However, Roy *et al.* (1986) suggested that β-oxidation can occur directly with unsaturated LCFA, based on observations made with *Syntrophomonas sapovorans*. Detection of palmitate (C16 : 1) as a product of linoleate (C18 : 2) degradation also suggested the latter (Lalman & Bagley, 2000). According to Lalman & Bagley (2001) production of shorter-chain LCFA from oleate and linoleate acid is energetically more favorable than from stearate. Nevertheless, from the 10 isolates known to be involved in syntrophic fatty acid degradation only three are able to use unsaturated-LCFA, namely, *Syntrophomonas sapovorans* (Roy *et al.*, 1986), *Thermosyntropha lipolytica* (Svetlitshnyi *et al.*, 1996) and *Syntrophomonas curvata* (Zhang *et al.*, 2004). This might be an indication that only some bacteria have the capability to degrade unsaturated LCFA and can also be an explanation for the differences found in the bacterial community fingerprints obtained from the samples under study. Clone lcfa_Bb13, which is related to *Syntrophomonas*-like organisms (Fig. 2a), appeared in samples after contact with oleate (SO and SO_b) and was virtually absent from samples after contact with palmitate (SP and SP_b). Conversely, other bacteria that clustered within the *Syntrophomonadaceae* appeared to be more predominant in samples after continuous palmitate feeding, e.g. clone lcfa_Bc53 and clone lcfa_Bb67.

No significant changes in the archaeal communities were observed during LCFA accumulation, indicating that composition of the archaeal microbiota remained rather stable (99.0% similarity between SO and SP). Archaea present in reactors RO and RP received the same end-products from oleate and palmitate degradation, i.e. acetate and hydrogen. In fact, their activity might be limited by the availability of these metabolites derived from complete oxidation of LCFA that is limited during the continuous feeding. Similarly, in both reactors, hydrogen and acetate are consumed by hydrogenophilic *Methanobacterium*-like and acetoclastic archaea related to *Methanosaeta*, respectively.

After continuous loading, the sludges containing associated LCFA (SO and SP) were incubated in batch assays and the accumulated substrate was efficiently mineralized (degradation step). A specific biomass-associated LCFA content of 4570 ± 257 and of 5200 ± 9 mg COD $gVSS^{-1}$ in sludge SO and SP, respectively, was converted to methane (Pereira *et al.*, 2005). During this process it is expected that bacteria involved in the β-oxidation of the accumulated-LCFA have a high activity together with the methanogenic partners. Bacterial DGGE profiles of sludge samples after batch degradation of the accumulated substrate, SO_b and SP_b, showed a lower number of predominant bands than those from samples SO and SP, indicating a decrease in the bacterial diversity (Fig. 1). This decreased diversity could be related to a functional specialization of the microbial community. Bacterial DGGE pattern similarity indices for sludge samples SO/SO_b and SP/SP_b were 60.7% and 74.6%, respectively. In addition, comparing SO_b and SP_b with sludge I, similarity indices of 22.1% and 24.5%, respectively, support the proposed changes in the bacterial consortium after being submitted to LCFA accumulation and degradation. Palmitate was the main LCFA accumulating onto the sludge during operation of reactor RO and the only LCFA detected in sludge present in reactor RP. During batch

incubation of sludges SO and SP this accumulated substrate is the only carbon and energy source present, and it is obviously similar for both samples. Despite that, the similarity index for the DGGE profiles from samples SO_b and SP_b is only 50.0%. This difference may reflect the changes that have occurred already during the first enrichment phase, associated with the continuous LCFA feeding to RO and RP. During continuous reactor operation, sludges SO and SP were fed with different substrates resulting in a different microbial composition (Fig. 1a). In fact, samples SO and SP showed already a relatively low similarity of 54% based on DGGE profiles. It is reasonable to assume that, after batch incubation, these differences are not completely reversible. It should, however, be considered that bacterial populations corresponding to predominant DGGE-bands in both samples (SO_b and SP_b) cluster within the same taxonomic groups indicating that their functions in the total ecosystem might be similar.

The archaeal profiles of both depleted sludges exhibited a lower similarity towards the respective LCFA-loaded sludge as compared to the bacterial microbiota (archaeal profile similarity indices for SO/SO_b and SP/SP_b were 37.0% and 6.2%, respectively), which was mainly due to the substitution of *Methanosaeta* by *Methanosarcina* species. During the continuous load, acetate was the only VFA detected in the effluent of both reactors, at an average concentration of 299.5 ± 103.5 and $72.7 \pm 33.5\ mg\ L^{-1}$, in RO and RP, respectively (Pereira *et al.*, 2005). Such low acetate concentrations were favorable for the dominance of *Methanosaeta*, which have a higher affinity for acetate (Jetten *et al.*, 1992). On the other hand, during batch degradation, the release of large amounts of acetate to the medium due to degradation of the biomass-associated LCFA might create favorable conditions for growth of *Methanosarcina*, which have a higher growth rate (Jetten *et al.*, 1992).

In the overall LCFA-accumulation/degradation process a majority of the analyzed bacterial clones (87%) clustered within the *Firmicutes*. A prevalence of organisms belonging to the *Clostridiaceae* and *Syntrophomonadaceae* suggests that these populations play an important role in LCFA degradation. Nevertheless, the achievement of pure culture isolates and their physiologic characterization would be important in order to better understand the metabolic function of these microorganisms in the ecosystem. In fact, a significant fraction of the retrieved 16S rRNA gene sequences were closely related to uncultured organisms (53% of the total sequences) indicating that follow-up studies should focus on the cultivation of LCFA-degrading organisms. On the contrary, methanogenic microorganisms present in all sludge samples are closely related to known hydrogen and acetate consumers. Some authors described an inhibitory effect of LCFA on acetoclastic methanogens (Hanaki *et al.*, 1981; Koster & Cramer, 1987; Angelidaki & Ahring, 1995; Lalman & Bagley, 2000, 2001). Inhibition of hydrogenotrophic methanogens by LCFA has been also reported (Demeyer & Henderic, 1967; Hanaki *et al.*, 1981; Lalman & Bagley, 2000, 2001), although much less severely. Conversely, it was reported by several authors that inhibition by LCFA is not permanent and adaptation of biomass to lipids/LCFA can occur (Broughton *et al.*, 1998; Alves *et al.*, 2001; Kim *et al.*, 2004; Pereira *et al.*, 2004). Pereira *et al.* (2005) have further showed that transport limitations, due to the accumulation of LCFA onto the sludge, largely contribute to the generally observed lag phases, normally ascribed to phenomena of inhibition or/and toxicity. Also, in the present study, the relative abundance of archaeal populations measured in different samples after contact with LCFA did not support significant inhibition. Moreover, previous results obtained for the same sludge samples had further shown that a significant increase in the specific methanogenic activity (SMA) towards acetate and H_2/CO_2 occurred after batch depletion of the LCFA accumulated onto the sludge (Pereira *et al.*, 2005).

The values obtained for archaea relative abundance were considerably lower when measured by FISH than by real-time PCR. These differences might be explained by the limitations of each of these methods, namely differences in rRNA-encoding *rrn* operon numbers and low membrane permeability, interfering with real-time PCR and FISH, respectively. Differences of 20–55% in the values of archaeal percentages measured by FISH and real-time PCR were also observed by Yu *et al.* (2005a) during archaea quantification in sludges from different anaerobic reactors. This variance in results using FISH and real-time PCR is in the same range of the variance observed in the present study.

In samples collected from reactors RO and RP (SO and SP) archaea represent $48 \pm 9.0\%$ and $35.4 \pm 14.3\%$ of the total microbial community, respectively, as measured by real-time PCR. The relative percentage of archaea in sample SP, measured as the ratio of cells hybridized with probe ARC915 and cells stained with DAPI, is lower, i.e. $19.1 \pm 1.4\%$. The values obtained in this work are inside the reported range for the archaea proportion found in several anaerobic reactors, although there has been a lack of data for LCFA-treating anaerobic systems. Tagawa *et al.* (2000) quantified archaeal communities present in 11 full- and lab-scale anaerobic reactors treating different kinds of wastewater, using probe ARC915. In those reactors, the ratio of hybridized cells accounted for 28–53% of the total DAPI-stained cells. Additionally, data by Tay *et al.* (2001) refers to an archaeal 16S rRNA gene proportion, determined by FISH, of 33% in sludge from an anaerobic reactor treating municipal wastewater. Other studies, using dot blot hybridization, report relative archaeal rRNA abundances of 46.7% in a reactor treating wastewater from a cheese factory

(Casserly & Erijman, 2003), and of 63% in a reactor treating paper-mill wastewater (Roest *et al.*, 2005).

After batch depletion of the accumulated-LCFA, the relative abundance of archaea increased significantly, as evaluated by both FISH and real-time PCR. This indicates that methanogenic organisms can endure after extensive contact with LCFA. In samples SO_b and SP_b the relative archaeal rRNA copies were as high as $85.3 \pm 28.9\%$ and $75.0 \pm 14.0\%$, respectively. During batch incubation of highly LCFA-loaded sludges, the acetate and hydrogen produced are likely to induce an increase in the methanogenic population. The proportion of archaeal 16S rRNA gene copies, determined by real-time PCR, was 72% in anaerobic sludge from a reactor fed with acetate (Sawayama *et al.*, 2006).

Molecular techniques for the study of microbial composition of samples subjected to LCFA-accumulation/degradation cycles provided important insight into the consortia involved in the degradation of these compounds. Members of the *Clostridiaceae* and *Syntrophomonadaceae* appeared pivotal to LCFA degradation. A combination of molecular approaches and cultivation may be necessary to better understand anaerobic LCFA-degradation. Archaeal populations, described as potentially vulnerable to the contact with LCFA, were able to survive to LCFA-accumulation/degradation steps.

Acknowledgements

The authors would like to acknowledge Mahmut Altinbas for the technical assistance with molecular techniques. The support of Frank de Bok and Mark Sturme with real-time PCR is gratefully appreciated. This study was financed by research grants of the Fundação para a Ciência e Tecnologia (FCT) and Fundo Social Europeu (FSE) attributed to D.Z. Sousa (SFRH/BD/8726/2002) and M.A. Pereira (SFRH/BPD/14591/2003).

References

Altschul SF, Gish W, Miller W, Meyers EW & Lipman DJ (1990) Basic local alignment search tool. *J Mol Biol* **215**: 403–410.

Alves MM, Vieira JA, Pereira RM, Pereira MA & Mota M (2001) Effects of lipids and oleic acid on biomass development in anaerobic fixed-bed reactors. Part II: oleic acid toxicity and biodegradability. *Water Res* **35**: 264–270.

Amann RI (1995) *In situ* identification of microorganisms by whole cell hybridization with rRNA-target nucleic acid probes. *Molecular Microbial Ecology Manual* (Akkermans ADL, van Elsas JD & de Bruijn FJ, eds), pp. 3.3.6/1–3. Kluwer Academic Publishers, Dordrecht.

Amann RI, Ludwig W & Schleifer KH (1995) Phylogenetic identification and *in-situ* detection of individual microbial cells without cultivation. *Microbiol Rev* **59**: 143–169.

Angelidaki I & Ahring BK (1992) Effects of free long-chain fatty acids on thermophilic anaerobic digestion. *Appl Microbiol Biotechnol* **37**: 808–812.

Angelidaki I & Ahring BK (1995) Establishment and characterization of an anaerobic thermophilic (55 °C) enrichment culture degrading long-chain fatty acids. *Appl Environ Microbiol* **61**: 2442–2445.

Broughton MJ, Thiele JH, Birch EJ & Cohen A (1998) Anaerobic batch digestion of sheep tallow. *Water Res* **32**: 1423–1428.

Casserly C & Erijman L (2003) Molecular monitoring of microbial diversity in an UASB reactor. *Int Biodeterior Biodegradation* **52**: 7–12.

Cole JR, Chai B, Marsh TL *et al.* (2003) The Ribosomal Database Project (RDP-II): previewing a new autoaligner that allows regular updates and the new prokaryotic taxonomy. *Nucleic Acids Res* **31**: 442–443.

Demeyer DI & Henderic HK (1967) Effect of C18 unsaturated fatty acids on methane production in vitro by mixed rumen bacteria. *Biochim Biophys Acta* **137**: 484–497.

Elberson MA & Sowers KR (1997) Isolation of an aceticlastic strain of *Methanosarcina siciliae* from marine canyon sediments and emendation of the species description for *Methanosarcina siciliae*. *Int J Syst Bacteriol* **47**: 1258–1261.

Grosskopf R, Janssen PH & Liesack W (1998) Diversity and structure of the methanogenic community in anoxic rice paddy soil microcosms as examined by cultivation and direct 16S rRNA gene sequence retrieval. *Appl Environ Microbiol* **64**: 960–969.

Hanaki K, Nagase M & Matsuo T (1981) Mechanism of inhibition caused by long-chain fatty acids in anaerobic digestion process. *Biotechnol Bioeng* **23**: 1591–1610.

Hane BG, Jager K & Drexler HG (1993) The Pearson product-moment correlation coefficient is better suited for identification of DNA fingerprint profiles than band matching algorithms. *Electrophoresis* **14**: 967–972.

Hedderich R & Whitman WB (2005) Physiology and biochemistry of methane-producing archaea. *The Prokaryotes: An Evolving Electronic Resource for the Microbiological Community* (Dworkin M, Falkow S, Rosenberg E, Schleifer K-H & Stackebrandt E, eds), pp. 1050–1079. Springer-Verlag, New York.

Hwu C-S (1997) Enhancing anaerobic treatment of wastewater containing oleic acid. PhD Thesis, Wageningen Agriculture University, the Netherlands.

Jackson BE, Bhupathiraju VK, Tanner RS, Woese CR & McInerney MJ (1999) *Syntrophus aciditrophicus* sp. nov., a new anaerobic bacterium that degrades fatty acids and benzoate in syntrophic association with hydrogen-using microorganisms. *Arch Microbiol* **171**: 107–114.

Jetten MSM, Stams AJM & Zehnder AJB (1992) Methanogenesis from acetate: a comparison of the acetate metabolism in

Methanothrix soehngenii and *Methanosarcina* spp. *FEMS Microbiol Rev* **88**: 181–197.

Kendall MM & Boone DR (2004) The order *Methanosarcinales*. *The Prokaryotes: An Evolving Electronic Resource for the Microbiological Community* (Dworkin M, Falkow S, Rosenberg E, Schleifer K-H & Stackebrandt E, eds), pp. 244–256. Springer-Verlag, New York.

Kim S-H, Han S-K & Shin H-S (2004) Two-phase anaerobic treatment system for fat-containing wastewater. *J Chem Technol Biotechnol* **79**: 63–71.

Koster IW & Cramer A (1987) Inhibition of methanogenesis from acetate in granular sludge by long-chain fatty acids. *Appl Environ Microbiol* **53**: 403–409.

Lalman JA & Bagley DM (2000) Anaerobic degradation and inhibitory effects of linoleic acid. *Water Res* **34**: 4220–4228.

Lalman JA & Bagley DM (2001) Anaerobic degradation and methanogenic inhibitory effects of oleic and stearic acids. *Water Res* **35**: 2975–2983.

Lane DJ (1991) 16S/23S rRNA sequencing. *Nucleic Acid Techniques in Bacterial Systematics* (Stackebrandt E & Goodfellow M, eds), pp. 142–175. John Wiley & Sons, Chichester.

Leclerc M, Delgenes JP & Godon JJ (2004) Diversity of the archaeal community in 44 anaerobic digesters as determined by single strand conformation polymorphism analysis and 16S rDNA sequencing. *Environ Microbiol* **6**: 809–819.

Ludwig W, Strunk O, Westram R *et al.* (2004) ARB: a software environment for sequence data. *Nucleic Acids Res* **32**: 1363–1371.

Ma K, Liu XL & Dong XZ (2006) *Methanosaeta harundinacea* sp. nov., a novel acetate-scavenging methanogen isolated from a UASB reactor. *Int J Syst Evol Microbiol* **56**: 127–131.

Manz W, Amann R, Ludwig W, Wagner M & Schleifer K-H (1992) Phylogenetic oligodeoxynucleotide probes for the major subclasses of proteobacteria: problems and solutions. *Syst Appl Microbiol* **15**: 593–600.

McInerney MJ (1992) The genus *Syntrophomonas*, and other syntrophic bacteria. *The Prokaryotes* (Balows A, Trüper HG, Dworkin M, Harder W & Schleifer KH, eds), pp. 2048–2057. Springer, New York.

Muyzer G, de Waal EC & Uitterlinden AG (1993) Profiling of complex microbial populations by denaturing gradient gel electrophoresis analysis of polymerase chain reaction-amplified genes coding for 16S rRNA. *Appl Environ Microbiol* **59**: 695–700.

Nübel U, Engelen B, Felske A, Snaidr J, Wieshuber A, Amann RI, Ludwig W & Backhaus H (1996) Sequence heterogeneities of genes encoding 16S rRNAs in *Paenibacillus polymyxa* detected by temperature gradient gel electrophoresis. *J Bacteriol* **178**: 5636–5643.

Pereira MA, Roest K, Stams AJM, Mota M, Alves M & Akkermans ADL (2002) Molecular monitoring of microbial diversity in expanded granular sludge bed (EGSB) reactors treating oleic acid. *FEMS Microbiol Ecol* **41**: 95–103.

Pereira MA, Cavaleiro AJ, Mota M & Alves MM (2003) Accumulation of long chain fatty acids onto anaerobic sludge under steady state and shock loading conditions: effect on acetogenic and methanogenic activity. *Water Sci Technol* **48**: 33–40.

Pereira MA, Sousa DZ, Mota M & Alves MM (2004) Mineralization of LCFA associated with anaerobic sludge: kinetics, enhancement of methanogenic activity, and effect of VFA. *Biotechnol Bioeng* **88**: 502–511.

Pereira MA, Pires OC, Mota M & Alves MM (2005) Anaerobic biodegradation of oleic and palmitic acids: evidence of mass transfer limitations caused by long chain fatty acid accumulation onto the anaerobic sludge. *Biotechnol Bioeng* **92**: 15–23.

Rinzema A, Boone M, van Knippenberg K & Lettinga G (1994) Bactericidal effect of long chain fatty acids in anaerobic digestion. *Water Environ Res* **66**: 40–49.

Roest K, Heilig HGHJ, Smidt H, de Vos WM, Stams AJM & Akkermans ADL (2005) Community analysis of a full-scale anaerobic bioreactor treating paper mill wastewater. *Syst Appl Microbiol* **28**: 175–185.

Roy F, Samain E, Dubourguier HC & Albagnac G (1986) *Synthrophomonas sapovorans* sp. nov., a new obligately proton reducing anaerobe oxidizing saturated and unsaturated long-chain fatty acids. *Arch Microbiol* **145**: 142–147.

Saitou N & Nei M (1987) The neighbor-joining method: a new method for reconstructing phylogenetic trees. *Mol Biol Evol* **4**: 406–425.

Sanguinetti CJ, Dias Neto E & Simpson AJ (1994) Rapid silver staining and recovery of PCR products separated on polyacrylamide gels. *BioTechniques* **17**: 914–921.

Sawayama S, Tsukahara K & Yagishita T (2006) Phylogenetic description of immobilized methanogenic community using real-time PCR in a fixed-bed anaerobic digester. *Bioresour Technol* **97**: 69–76.

Schink B (1997) Energetics of syntrophic cooperation in methanogenic degradation. *Microbiol Mol Biol Rev* **61**: 262–280.

Stahl DA & Amann R (1991) Development and application of nucleic acid probes. *Nucleic Acid Techniques in Bacterial Systematics* (Stackebrandt E & Goodfellow M, eds), pp. 205–248. John Wiley & Sons, Chichester.

Svetlitshnyi V, Rainey F & Wiegel J (1996) *Thermosyntropha lipolytica* gen. nov., sp. nov., a lipolytic, anaerobic, alkalitolerant, thermophilic bacterium utilizing short- and long-chain fatty acids in syntrophic coculture with a methanogenic archaeum. *Int J Syst Bacteriol* **46**: 1131–1137.

Tagawa T, Syutsubo K, Sekiguchil Y, Ohashi A & Harada H (2000) Quantification of methanogen cell density in anaerobic granular sludge consortia by fluorescence in-situ hybridization. *Water Sci Technol* **42**: 77–82.

Tay TLS, Ivanov V, Kim IS, Feng L & Tay JH (2001) Quantification of ratios of Bacteria and Archaea in methanogenic microbial community by fluorescence in situ hybridization and

fluorescence spectrometry. *World J Microbiol Biotechnol* **17**: 583–589.

Wallner G, Amann R & Beisker W (1993) Optimizing fluorescent *in situ* hybridization with rRNA-targeted oligonucleotide probes for flow cytometric identification of microorganisms. *Cytometry* **14**: 136–143.

Weng C & Jeris JS (1976) Biochemical mechanisms in methane fermentation of glutamic and oleic acids. *Water Res* **10**: 9–18.

Wu C, Liu X & Dong X (2006) *Syntrophomonas erecta* subsp. *sporosyntropha* subsp. nov., a spore-forming bacterium that degrades short chain fatty acids in co-culture with methanogens. *Syst Appl Microbiol* **29**: 457–462.

Yu Y, Lee C & Hwang S (2005a) Analysis of community structures in anaerobic processes using a quantitative real-time PCR method. *Water Sci Technol* **52**: 85–91.

Yu Y, Lee C, Kim J & Hwang S (2005b) Group-specific primer and probe sets to detect methanogenic communities using quantitative real-time polymerase chain reaction. *Biotechnol Bioeng* **89**: 670–679.

Zhang CY, Liu XL & Dong XZ (2004) *Syntrophomonas curvata* sp. nov., an anaerobe that degrades fatty acids in co-culture with methanogens. *Int J Syst Evol Microbiol* **54**: 969–973.

Zhao H, Yang D, Woese CR & Bryant MP (1993) Assignment of fatty acid-b-oxidizing syntrophic bacteria to *Syntrophomonadaceae* fam. nov. on the basis of 16S rRNA sequence analysis. *Int J Syst Bacteriol* **43**: 278–286.

Zheng D & Raskin L (2000) Quantification of *Methanosaeta* species in anaerobic bioreactors using genus- and species-specific hybridization probes. *Microb Ecol* **39**: 246–262.

Zoetendal EG, Akkermans ADL, Akkermans Van Vliet WM, de Visser JAGM & de Vos WM (2001) The host genotype affects the bacterial community in the human gastrointestinal tract. *Microb Ecol Health Dis* **13**: 129–134.